analytical chemistry

Letter

pubs.acs.org/ac

Enzymatic and Nonenzymatic Electrochemical Interaction of Abiraterone (Antiprostate Cancer Drug) with Multiwalled Carbon Nanotube Bioelectrodes

Nima Aliakbarinodehi,* Giovanni De Micheli, and Sandro Carrara

Integrated Systems Laboratory, École Polytechnique Fédérale de Lausanne (EPFL), Lausanne, Switzerland 1015

ABSTRACT: Unexplored electrochemical behavior of abiraterone, a recent and widely used prostate cancer drug, in interaction with cytochrome P450 3A4 (CYP3A4) enzyme and multiwalled carbon nanotubes (MWCNTs) is investigated in this work. The results reported in this work are significant for personalized medicine and point-of-care chemical treatment, especially to improve the life expectancy and quality of life of patients with prostate-cancer. To this purpose, enzymatic and nonenzymatic electrochemical biosensors were developed and characterized with different concentrations of abiraterone. Nonenzymatic biosensors were functionalized with MWCNTs as a catalyst for signal enhancement, while enzymatic biosensors have been obtained with CYP3A4 protein immobilized on MWCNTs as recognition biomolecule. Enzymatic electrochemical experiments demonstrated an inhibition effect on the CYP3A4, clearly observed as a diminished electrocatalytic activity of the enzyme. Electrochemical responses of nonenzymatic biosensors clearly demonstrated the direct electroactivity of abiraterone when reacting with MWCNT as well as an electrode-fouling effect.

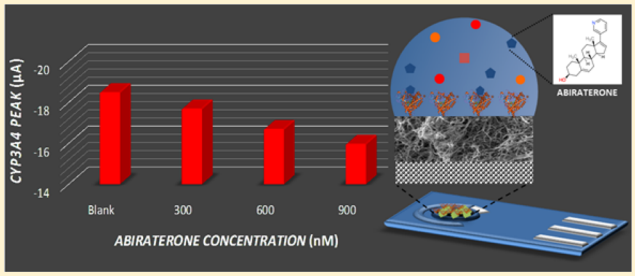

Abiraterone chemotherapy is a type of hormone therapy for patients suffering from metastasized castration-resistant prostate cancer. Administration of this agent causes testosterone suppression, and thus, shrinking the number of testosterone-sensitive tumor cells all over the body. Mechanism of action is based on the inhibition of steroidogenic enzyme "17α-hydroxylase/C17, 20 lyase (CYP17A1)" that catalyzes the 17α-hydroxylation of pregnenolone and progesterone and subsequent formation of dehydroepiandrosterone and androstenedione, as precursors of testosterone.[1]

Abiraterone is now widely used for chemotherapy-naive patients or patients treated by docetaxel. The therapeutic range is in the range between 20 nM and 360 nM for a typical dose of 1000 mg injected per day.[2] Such a dose is the right one to maintain the concentration of abiraterone in this range and, therefore, to achieve a successful chemotherapy, since lower concentration cannot provide a medical benefit and higher concentrations will cause severe side effects due to overdosing. Therapeutic drug monitoring by means of point-of-care electrochemical biosensors would help the patients to achieve this goal. However, a proper knowledge of the drug electrochemistry is essential for development of any electrochemical biosensor while, at the best of our knowledge, the full electrochemical characterization of the abiraterone has not yet been published in the literature. Therefore, the electrochemical response of abiraterone in interaction with CYP3A4 and MWCNT is proposed in this work.

EXPERIMENTAL SECTION

Macro screen-printed electrodes (SPEs) are purchased from Metrohm (DRP-110). Powder of MWCNTs (diameter, 10 nm; length, 1−2 μm; 90% purity) was purchased from DropSens (Spain). These MWCNTs were 5% functionalized with COOH to facilitate the suspension in solvent. They were dispersed in chloroform to the concentration of 1 mg mL^{-1} and were sonicated for 1 h to achieve a stable homogeneous solution. Phosphate buffer saline (PBS; 100 mM; pH 7.4) was provided by Sigma-Aldrich, solvated in distilled water, and stirred to obtain the homogeneous solution. It was used as a supporting electrolyte in all experiments. Abiraterone powder was purchased from Medchemtronica (Stockholm, Sweden) and was dissolved in dimethyl sulfoxide (DMSO) buffer to the concentration of 10 mM to be used as a stock solution. CYP3A4, purified and microsomal, (pureCYP3A4, micrCYP3A4) was purchased from Sigma-Aldrich and was stored at −80 °C. Microsomes contain recombinant human CYP3A4 and cytochrome P450 reductase proteins (CYP-reductase). Enzymes were used as received.

Commercially available SPEs were used to fabricate the biosensors. The SPEs present carbon working electrode (WE, area 0.12 cm^2), carbon counter electrode, and silver reference electrode. Functionalization of SPEs with MWCNTs was carried out by the drop-casting technique.[3] In the drop casting procedure, 20 μL of MWCNT dispersion (in steps of 4 μL)

Received: July 18, 2016
Accepted: September 14, 2016
Published: September 14, 2016

DOI: 10.1021/acs.analchem.6b02747
Anal. Chem. 2016, 88, 9347−9350

were dropped over the working electrode by pipet and allowed to dry after each step. Final electrode was stable and robust, as MWCNTs were attached over the WE by van der Waals and hydrophobic interactions. After MWCNTs nanostructuring (20 μg of nanomaterial), the final electroactive surface area resulted enhanced by 4314 mm^2.[3,4] Nanostructured SPEs were then stored at ambient temperature. Bare or nanostructure carbon WE were coated by 9 μL of CYP3A4 enzymes and incubated at +4 °C overnight to immobilize the biomolecules on the surface. This provides specificity to the surface by adding the recognition element of the biosensors.[5] Then, the electrodes were washed with distilled water to remove any unbound biomolecules and further covered by PBS and stored at +4 °C for further use. CYP450 are immobilized over the MWCNTs through physical adsorption without altering their shape or attenuating their catalytic activity. The main reason is that MWCNTs form a 3D porous structure over the surface that provides a large effective surface area (compared to a not nanostructured surface) for CYP450 protein adsorption.

An Autolab potentiostat/galvanostat (PGSTAT128N, Metrohm, The Netherlands) was used for cyclic voltammetry (CV) under aerobic conditions. To acquire the CV responses (voltammograms), bioelectrodes were immersed in a beaker containing 10 mL of buffer, gently stirred. This stirring will help to maintain the redox environment and assures that the observed response is due to the drug−enzyme reaction. For different concentrations of drug, an adequate amount of abiraterone stock solution (10 mM in DMSO buffer) was added to the beaker solution. The potential was scanned between −0.8 V and +0.6 V vs Ag, for 10 cycles (to obtain stable response), at a scan rate of 70 mV per second. Voltammograms were analyzed with the Nova Software (Metrohm) for baseline correction and removing the faradaic current from the capacitive background. Reduction peaks were considered for investigation having performed the acquisitions in the presence of oxygen. For data interpretation, a suitable baseline was set for the faradaic current of the reduction peaks. A typical voltammograms obtained in this work and the corrected baseline is illustrated in Figure 1.

ELECTROCHEMICAL RESULTS AND DISCUSSION

Electrochemical analysis started with the identification of different peaks detected on the voltammograms. Several different biosensors were fabricated by changing the nanostructuring and enzyme in the biofunctionalization of SPEs, including carbon electrode biofunctionalized with micrCYP3A4 (carbon/micrCYP3A4), MWCNT nanostructured electrodes biofunctionalized with micrCYP3A4 (carbon/MWCNT/micrCYP3A4), MWCNT nanostructured electrodes biofunctionalized with pureCYP3A4 (carbon/MWCNT/pureCYP3A4), and not biofunctionalized MWCNT nanostructured electrodes (carbon/MWCNT).

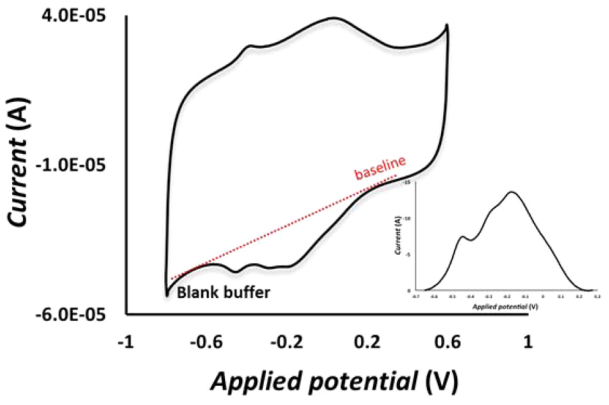

Figure 1. Typical voltammograms obtained for enzymatic monitoring of abiraterone. Inset shows the acquired faradaic peaks after baseline correction and capacitive current removal.

Four reduction peaks were clearly observed in the response of abiraterone and CYP3A4 interaction: they are located at −430 mV, −270 mV, −140 mV, and 61 mV. In order to identify these peaks, electrochemical responses of different biosensors working on 900 nM drug solutions were compared (Figure 2). These peaks were identified by comparing the

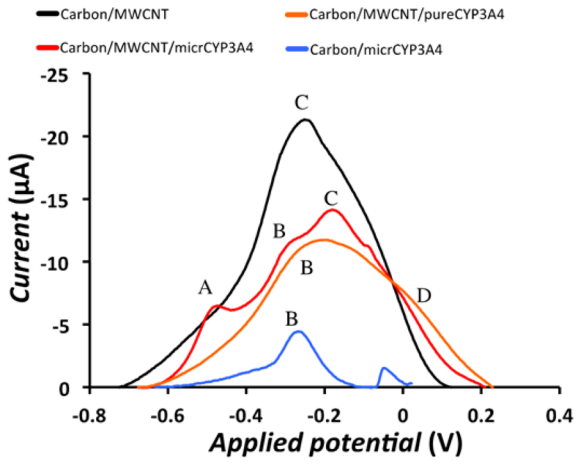

Figure 2. Identification of electrochemical peaks related to interaction of abiraterone with CYP3A4 and MWCNTs.

response of these different realized biosensors with each other and with independent observation published in the literature by other authors.[6] Comparison of behavior in the presence and absence of abiraterone is presented in Figure 3a,b.

The analysis of those peaks shows that (A) The first peak (−430 mV) was recorded just for biosensors with micrCYP3A4. It did not exist on voltammograms of carbon/MWCNT, so it is related to biomolecules. Moreover, it does not appear on voltammograms related to pureCYP3A4-based biosensors, so it belongs to CYP-reductase molecules that coexist with CYP3A4 protein in the microsome. (B) The second peak (−270 mV) belongs to CYP3A4 protein, also confirmed by the fact that it was observed in the response of all CYP3A4 based biosensors. (C) The third peak (−140 mV) appears for just the nanostructured biosensors but not on the response of carbon/micrCYP3A4 biosensors. Therefore, it is identified as the MWCNTs peak. (D) The fourth peak (61 mV) was increasing over time and was stabilized with increasing the number of cycles, so it was identified as a background peak, as also confirmed by our group in other similar electrochemical systems.[6]

The inhibition of CYP3A4 by increasing the concentration of abiraterone was observed in voltammograms acquired by carbon/MWCNT/micrCYP3A4 biosensor. The CYP3A4 faradaic peak (−270 mV) is related to the reduction of the active site of the enzyme (heme group). This peak would increase/decrease in the presence of a substrate/inhibitor of the enzyme. The acquired response of biosensor to 300 nM, 600 nM, and 900 nM abiraterone showed a gradual inhibition and

DOI: 10.1021/acs.analchem.6b02747
Anal. Chem. 2016, 88, 9347−9350

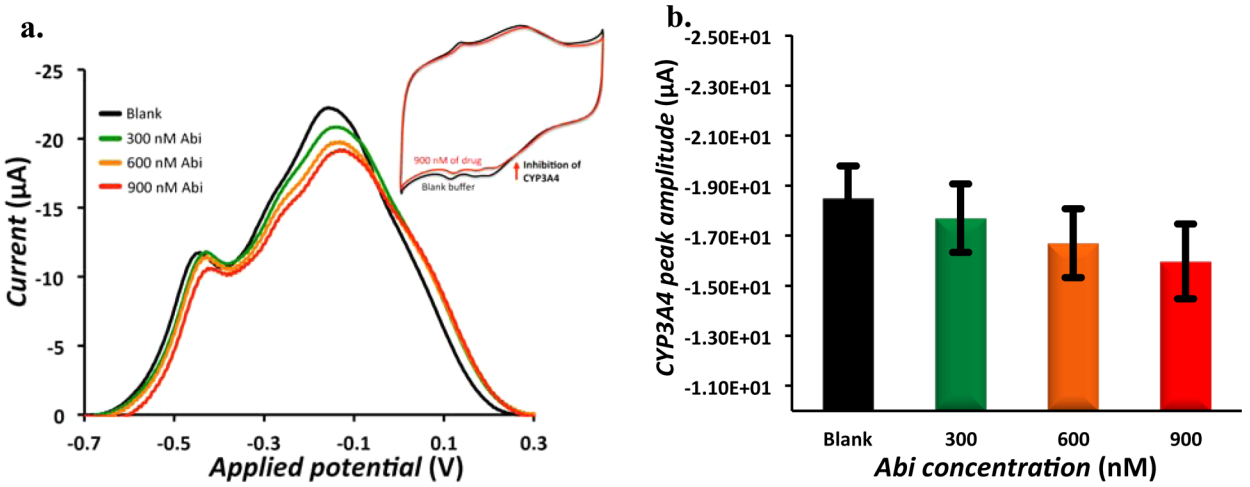

Figure 3. Gradual inhibition of CYP3A4 catalytic activity by increasing abiraterone concentration; inset shows a complete voltammograms in buffer and after interaction with 900 nM abiraterone (a). Averaged reduction peak of CYP3A4 at different drug concentrations; error bars are standard error of triplicate measurements (b).

suppression of catalytic activity of CYP3A4. Reduction peaks are presented in Figure 3a, and their measured amplitudes are presented in Figure 3b for comparison. This inhibition reaction can be explained by the chemical structure of the drug and its interaction with enzyme molecules on the surface.

The abiraterone structure harbors three main features, including the aromatic nitrogen-containing heterocycle (pyridine moiety), the hydrophobic steroidal core, and the hydroxyl group that together ends the high affinity of the drug for irreversible binding to cytochrome P450 enzymes.[7−10] This inhibition, which is mainly due to the complexation of the Fe^{2+} of the heme group of CYP3A4 and the sp^2-hybridized nitrogen that exists in the pyridyl group, is described already in the literature.[9,11] However, this is the first time that this phenomena is presented utilizing electrochemical techniques. The redox reaction of CYP3A4 follows the Randles-Sevcik equation that explains current depends directly on the scan rate. The scan rate used in this work was 70 mV per second that was optimized for MWCNTs-based biosensors elsewhere.[4] Higher scan rates would increase the current amplitude but not the sensitivity of the biosensor to various abiraterone concentrations. At very high scan rates, current would not change as a function of scan rate, as current could not keep up with voltage changes.

Dose−response curve of carbon/MWCNT/micrCYP3A4 in interaction with a wide range of abiraterone concentrations was obtained to further investigate the effect of drug on the catalytic activity of CYP3A4 (Figure 4).

A clear inhibition of CYP3A4 was observed in the response as diminishing its reduction peak by increasing the drug concentration. Dose−response curve also presented two significant properties of this reaction. First, an exponential decay of the CYP3A4 peak was observed for drug concentrations between 0 and 1 μM. This range completely covers the therapeutic range of the targeted drug (therapeutic range is up to 360 nM), and this proves the capability of carbon/MWCNT/micrCYP3A4 for abiraterone concentration monitoring after proper optimization of the sensing system. Furthermore, by increasing the concentration from 1 μM to 3 μM, suppression of the reduction peak was saturated that was caused by irreversible inhibition of a majority of CYP3A4 proteins after reaction with abiraterone concentrations beyond 1 μM.

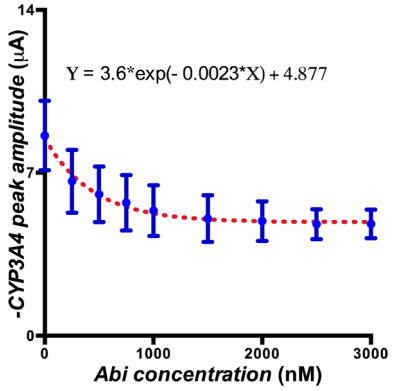

Figure 4. Dose−response curve of abiraterone in interaction with CYP3A4. The fitting equation is indicated.

Error bars in the figure indicate the intrasensors variations (averaged RSD = 36%), as each data point is an average of triplicate measurements carried out on three biosensors. The main source of response variations is the biosensor development procedure including nanostructuring and enzyme immobilization by van der Waals and hydrophobic forces. This procedure helped us to avoid complexity and focus on the behavior of the drug and the sensing surface. However, optimization of the biosensor for abiraterone detection will be the subject of this group's future work. The data points follow an exponential decay equation (eq 1), where Y_0 = 8.482 μA is the starting point, Plateau = 4.877 μA is the saturation region, and K = 0.002263 has the reciprocal of the X-axis unit (1/nM).

$$Y = (Y_0 - \text{Plateau})e^{-KX} + \text{Plateau} \quad (1)$$

Electrochemical interaction of abiraterone with MWCNT without involvement of any enzyme caused an increment of the MWCNT peak, as is demonstrated in Figure 5. This proved the direct electron transfer between the drug and MWCNT. In these experiments, response of carbon/MWCNT in blank buffer and 30 μM solution was recorded. A high drug concentration was used in this experiment to accelerate the fouling effect and make it more observable. Then electrodes

DOI: 10.1021/acs.analchem.6b02747
Anal. Chem. 2016, 88, 9347−9350

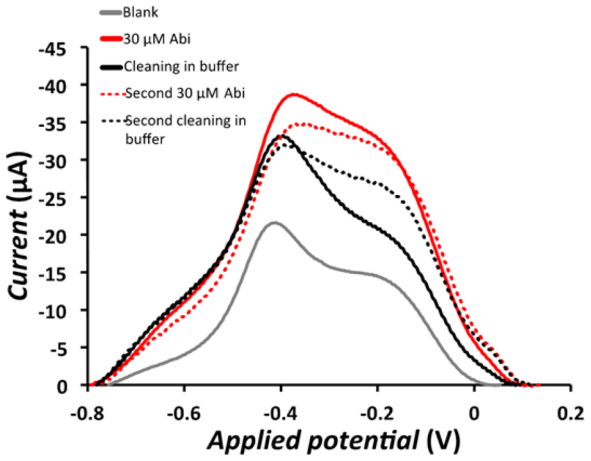

Figure 5. Direct electrochemical response of abiraterone and MWCNTs and the electrode-fouling effect caused by attachment of drug molecules on the surface.

were washed with distilled water and remeasured in blank buffer. This procedure was repeated several times. Acquired results (Figure 5) showed 15 μA increment of MWCNT peak after interaction with abiraterone with respect to blank buffer. The peak was reduced for only 5 μA in buffer after the washing while the original blank measure was 20 μA smaller. This demonstrates that the drug remained attached to the surface of the MWCNTs after the electron exchange. Furthermore, a stable response of ~32 μA was observed at the second cycle of the experiment. This shows that the surface was covered with drug residues that prevented the signal to be increase to the previous detected amount for drug detection and even prevented the signal to be reduced after washing to the previous recorded amplitude in blank buffer.

CONCLUSION

In this work, the electrochemical characterization of abiraterone in interaction with CYP3A4 enzyme and MWCNTs were investigated. Electrochemical responses of enzymatic biosensors exhibited inhibitory effect of abiraterone on CYP3A4 proteins. Besides, comparing the responses of various biosensors functionalized with different nanostructures and biomolecules identified the electrochemical peaks appeared in the responses of abiraterone: −430 mV for CYP-reductase, −270 mV for CYP3A4, −140 mV for MWCNTs, and 61 mV as background peak. Enzymatic electrochemical responses (Figures 3 and 4) presented an exponential decay until 1 μM that is consistent with abiraterone therapeutic range in the human body. This inhibition behavior saturates at concentrations around 3 μM. Complete detection of abiraterone is the subject of this group's future work. On the other hand, a direct electron transfer between abiraterone molecules and MWCNTs was recorded as well. Electrode-fouling phenomena was also observed in this direct interaction of the drug and MWCNTs that was the result of drug molecules attached on the surface. Therefore, abiraterone is classified as electroactive drug molecules with electrode-fouling characteristics.

AUTHOR INFORMATION

Corresponding Author

*E-mail: nima.aliakbarinodehi@epfl.ch.

Author Contributions

The manuscript was written through contributions of all authors. All authors have given approval to the final version of the manuscript.

Notes

The authors declare no competing financial interest.

ACKNOWLEDGMENTS

This research was supported partly by the Project PROSENSE funded by the European Union's Horizon 2020 Research and Innovation Programme under the Grant Agreement No. 317420 and partly by Grant ERC-2009-AdG-246810.

REFERENCES

(1) Hakki, T.; Bernhardt, R. *Pharmacol. Ther.* **2006**, *111*, 27−52.
(2) Acharya, M.; Bernard, A.; Gonzalez, M.; Jiao, J.; De Vries, R.; Tran, N. *Cancer Chemother. Pharmacol.* **2012**, *69*, 1583−1590.
(3) Aliakbarinodehi, N.; Taurino, I.; Pravin, J.; Tagliaferro, A.; Piccinini, G.; De Micheli, G.; Carrara, S. *Chem. Pap.* **2015**, *69*, 134−142.
(4) Aliakbarinodehi, N.; De Micheli, G.; Carrara, S. In *2015 11th Conference on Ph.D. Research in Microelectronics and Electronics (PRIME)*; Glasgow, U.K., June 29−July 2, 2015; pp 25−28.
(5) Baj-Rossi, C.; Micheli, G. D.; Carrara, S. *Sensors* **2012**, *12*, 6520−6537.
(6) Baj-Rossi, C.; Müller, C.; von Mandach, U.; De Micheli, G.; Carrara, S. *Electroanalysis* **2015**, *27*, 1507−1515.
(7) Yin, L.; Hu, Q. *Nat. Rev. Urol.* **2014**, *11*, 32−42.
(8) Hu, Q.; Yin, L.; Jagusch, C.; Hille, U. E.; Hartmann, R. W. *J. Med. Chem.* **2010**, *53*, 5049−5053.
(9) Pinto-Bazurco Mendieta, M. A.; Negri, M.; Jagusch, C.; Müller-Vieira, U.; Lauterbach, T.; Hartmann, R. W. *J. Med. Chem.* **2008**, *51*, 5009−5018.
(10) DeVore, N. M.; Scott, E. E. *Nature* **2012**, *482*, 116−119.
(11) Deb, S.; Chin, M. Y.; Adomat, H.; Guns, E. S. T. *J. Steroid Biochem. Mol. Biol.* **2014**, *144*, 50−58.

DOI: 10.1021/acs.analchem.6b02747
Anal. Chem. 2016, 88, 9347−9350